AAEC/E649

AUSTRALIAN ATOMIC ENERGY COMMISSION

RESEARCH ESTABLISHMENT

LUCAS HEIGHTS RESEARCH LABORATORIES

MICROSTRUCTURAL ASPECTS OF SYNROC FROM SANDIA PRECURSOR

2. SOME EFFECTS OF IMPURITIES

by

G. T. STEVENS

K. G. WATSON

A. BELLROSE

APRIL 1987

ISBN 0 642 59856 8

AUSTRALIAN ATOMIC ENERGY COMMISSION
RESEARCH ESTABLISHMENT

LUCAS HEIGHTS RESEARCH LABORATORIES

MICROSTRUCTURAL ASPECTS OF SYNROC FROM SANDIA PRECURSOR

2. SOME EFFECTS OF IMPURITIES

BY

G T STEVENS

K G WATSON

A BELLROSE

ABSTRACT

A description is given of the effects of small amounts of certain elements (Si, Na, P, Fe, Cl, F and S), which could be considered to be processing contaminants, on the microstructure of a particular batch of Synroc C.

National Library of Australia card number and ISBN 0 642 59856 8

The following descriptors have been selected from the INIS Thesaurus to describe the subject content of this report for information retrieval purposes. For further details please refer to IAEA-INIS-12 (INIS: Manual for Indexing) and IAEA-INIS-13 (INIS: Thesaurus) published in Vienna by the International Atomic Energy Agency.

CALCINATION; CHLORINE; EXPERIMENTAL DATA; FLUORINE; HOT PRESSING; IMPURITIES; IRON; MICROSTRUCTURE; PHOSPHORUS; RADIOACTIVE WASTE PROCESSING; RUTILE; SILICON; SODIUM; SULFUR; SYNROC PROCESS; SYNTHETIC ROCKS; TITANIUM OXIDES; X-RAY EMISSION ANALYSIS

EDITORIAL NOTE

From 27 April 1987, the Australian Atomic Energy Commission (AAEC) is replaced by Australian Nuclear Science and Technology Organisation (ANSTO). Serial numbers for reports with an issue date after April 1987 have the prefix ANSTO with no change of the symbol (E, M, S or C) or numbering sequence.

CONTENTS

1. INTRODUCTION

Synroc is a multi-phase, fine-grained polycrystalline titanate ceramic intended for the immobilisation of high-level waste (HLW) from the nuclear power industry. To be successful, the Synroc must immobilise the actinides and fission products from the nuclear fuel and also accommodate the residual process chemicals. Since the process chemistry varies according to local conditions, it is necessary to establish tolerance limits of the Synroc for a range of processing chemicals.

This report summarises the effects of certain elements, which could be considered to be processing contaminants, on the microstructure of a particular batch of Synroc (Sandia RE 15642). It is the second in a series of reports dealing with the optical and scanning electron microscope (SEM) evaluation of Sandia Synroc. The first report presented typical microstructures and showed the effects of altering certain process variables on the microstructure [Stevens *et al.* 1987].

Synroc consists of a fine grained matrix containing the following nominal phases:

(i) barium hollandite ($BaAl_2Ti_6O_{16}$),

(ii) perovskite ($CaTiO_3$),

(iii) zirconolite ($CaZrTi_2O_7$),

(iv) rutile (TiO_2), and

(v) metallic alloy (*e.g.* Mo, Pd, Ru, Fe).

The matrix also contains a dispersion of porous titanium oxide regions resulting from the addition of 2% Ti metal oxygen getter. These are referred to as Ti (oxide) relics.

The appearance of the microstructure in the SEM is determined by the morphology of the darker rutile or titanium oxide-based phase. The matrix titanium oxide varies from small equi-axed grains through chains of grains and irregular extended crystals to quite well developed acicular crystals. In the selected batch of Sandia, the mixed (irregular and sharp) acicular structure is common. The other matrix phases show no similar variation and are generally fine, equi-axed grains below one micrometre in diameter.

The factors determining the matrix titanium oxide morphology presumably include pressing temperature and composition as well as redox potential. The previous work indicated that the sharp acicular crystallites are favoured by pressing temperatures of 1200°C and below.

2. EXPERIMENTAL

The processing and experimental techniques have been described elsewhere [Stevens *et al.* 1987]. The elements Cl, F, Fe, Na, P, S and Si were evaluated over a range of concentrations and in selected combinations. Only one batch of material was prepared for each condition. Details of the concentrations are given in **table 1**. These elements were incorporated in the slurry after the 10% addition of simulated HLW. The material was dried, calcined at 750°C, then pressed at 1200°C and 14 MPa with a 2% metallic Ti getter. Some of the elements, notably Cl, F and S, may be volatilised during processing and thus may not be retained in the Synroc at the nominated concentrations.

3. RESULTS

The results are summarised in **table 2** and representative microstructures, with X-ray emission spectra (XES) where appropriate, are given in **figures 1-14**. In most cases, the impurities have affected the microstructure both by apparently altering the morphology of the matrix titanium oxide (rutile) and by forming new microconstituents:

(i) SiO_2 - At low levels, this impurity probably had little effect on the matrix, although at 0.2% the acicular rutile form was predominant. At 1%, the matrix was transformed by coarse colonies of rutile crystals similar to those found in Synroc pressed at around 1300°C. Small dark Si- and Al-rich microconstituents were detected at all levels.

(ii) Na_2O - At 1%, the matrix titanium oxide tended to be fine equi-axed grains uniformly distributed. With increasing levels of Na_2O, these grains became larger and definitely equi-axed. The matrix also contained a fine acicular phase of dark SEM contrast. This acicular phase is a calcium

aluminium titanate which has often been identified as hibonite, Ca (Ti, Al)$_{12}O_{19}$ [P.F. Fielding and T.J. White, private communication.]. No regions of Na segregation were found.

(iii) $SiO_2 + Na_2O$ - At the lowest levels, colonies of coarsely aligned rutile crystals were associated with the Ti (oxide) relics. The growth of unusually large grains in ceramic bodies during hot-pressing involves the formation of mobile grain boundaries (possibly liquid films), so it is possible that with this particular composition, at the particular pressing temperature, the extra heat from the oxidation of the Ti particles was sufficient to allow rapid titanium oxide grain growth. At higher levels, the association was not observed; instead, these specimens contained regions of high Si content surrounded by an annulus of coarse rutile and fine dark equi-axed grains containing Si, Na and Al. The latter were also found in the matrix.

(iv) P_2O_5 - This impurity had no significant effect on matrix rutile. Phosphorus was detected in small dark grains.

(v) Fe_2O_3 - This appeared in matrix titanium oxide as uniformly fine equi-axed grains. Metallic alloys were high in Fe.

(vi) $SiO_2 + Na_2O + P_2O_5 + Fe_2O_3$ - This combination caused the matrix to be equi-axed but non-uniform, with titanium oxide grains ranging in size up to about five micrometres. Phosphorus was detected in small dark grains which formed clusters. Metallic alloys were high in Fe.

(vii) Cl - Chlorine had no significant effect.

(viii) F - In the presence of fluorine, small dark Al-rich crystals occurred at all levels. At the higher levels, there was significant fine porosity concentrated around the outside of original calcine granules and the titanium (oxide) relics. Prismatic crystals of a Ti + Al phase and a zone depleted of matrix rutile were associated with the porosity. Fluorine was not detected in any of these microconstituents when using either EDS or wavelength dispersive spectroscopy on a Cameca CAMEBAX electron-probe microanalyser (courtesy of Dr D French, CSIRO) with a detection limit of about 0.1%.

(ix) SO_4 - This component had no significant effect.

4. DISCUSSION

The new phases or microconstituents introduced by the impurities and their elements are listed in table 3, together with a tentative mineral identification based on X-ray diffraction and transmission electron microscope studies by T.J. White.

All additives except Cl and SO_4 had an effect on the microstructure. In the case of Cl and SO_4, it is emphasised that they were added to the feed at very low levels (0.1% max.), so it is perhaps not surprising that no effect was detected. Silicon (with Al), P and F (Al only detected) gave rise to small discrete crystals, and most other additions affected the matrix titanium oxide morphology in some way.

In two specimens containing silicon, the matrix rutile was present as colonies of coarsely aligned crystals. This effect had been observed previously after pressing at around 1290°C, and is presumably due to the formation of mobile grain boundaries or liquid films at the boundaries. Since these experiments did not involve duplicate tests, in the absence of systematic trends there is a possibility that this effect was due to experimental error, *i.e.* the pressing temperature was too high, rather than to an effect of the Si impurity. Nevertheless, the coarse rutile crystals bordering the Si segregations in the higher SiO_2/Na_2O specimens are an indication of increased grain boundary mobility.

Sodium had a pronounced effect on the matrix titanium oxide. At all levels, the normal mixed acicular morphology is replaced with a mixture of a fine equi-axed phase and fine crystals of the Al-rich hibonite. Hibonite had been detected in earlier experiments in which the metallic getter was omitted or the Ti replaced with Fe or Ni. The grain size of the equi-axed phase increased with increasing Na content. Iron also replaced the acicular morphology with an equi-axed Ti oxide but there was only a trace of hibonite. When added in combination, the effects of Si, Na, Fe and P seemed to be additive.

Fluorine had an unusual effect. It apparently encouraged the formation of small Al-rich crystals throughout the structure, but around the outside of the original calcine granules this Al-rich phase was replaced by a Ti-Al phase. The migration of Ti to this new phase left the surrounding matrix porous and depleted of Ti.

5. CONCLUSIONS

The small amounts of Si, Na, P, Fe and F had an effect on the Synroc microstructure. No effect from the addition of Cl and SO_4 was detected at the very low level of 0.1% maximum. New discrete phases were formed by Si (with Al), P and F (Al only detected) but most other additions affected the morphology of the titanium oxide phase of the Synroc matrix.

6. ACKNOWLEDGEMENT

The samples were prepared by W Buykx.

7. REFERENCE

Stevens, G.T., Watson, K.G., Bellrose, A. [1987] - Microstructural aspects of Synroc from Sandia precursor. 1. Some effects of process variables. AAEC/E648.

TABLE 1
SPECIMEN DETAILS

Impurity	Concentrations (wt%)	Form Added to Slurry
SiO_2	0.2, 0.4, 1.0	Fumed silica
Na_2O	1.0, 2.5, 4.0	NaOH
SiO_2/Na_2O	0.2/1.0, 0.4/2.5, 1.0/4.0	
P_2O_5	1.0	H_3PO_4
Fe_2O_3	2.0	$Fe(N0_3)_3.9H_20$
$SiO_2/Na_2O/P_2O_5Fe_2O_3$	0.2/1.0/1.0/2.0	
Cl^-	0.02, 0.05, 0.1	NH_4Cl
F^-	0.02, 0.05, 0.1	NH_4F
SO_4^{2-}	0.02, 0.05, 0.1	$(NH_4)_2SO_4$

TABLE 2
SUMMARY OF RESULTS

Impurity (wt%)	Microconstituents	Fig. No.	Major Elements
Nil	Matrix rutile as irregular needles	1	
0.2 SiO_2	Matrix rutile in acicular form		Si,Al
	Dark inclusions about 1 µm across		
0.4 SiO_2	Matrix rutile as irregular needles		Si
	Dark inclusions		
1.0 SiO_2	Matrix rutile principally as aligned colonies of coarse crystals	2	Ti
	Dark crystals several micrometres across	3	Si,Al
1.0 Na_2O	Matrix rutile tending to equi-axed grains about 1 µm across.		
	Fine dark needles		
2.5 Na_2O	As above, rutile grains now 2 µm across; longer fine dark needles		
4.0 Na_2O	As above, rutile grains now up to 3 µm across	4	
	Larger dark needles	4	Al,Ti
0.2 SiO_2	Matrix rutile as fairly sharp needles		
1.0 Na_2O	Colonies of aligned coarse rutile crystals associated with titanium (oxide) relics		
0.4 SiO_2	Annular regions visible in optical microsc.	5	
2.5 Na_2O	Matrix rutile fine mixed acicular and equi-axed. Centre of annulus rutile-free	6	Si
	Coarser rutile crystals (up to 5 µm long) forming annulus		Ti
	Fine dark equi-axed crystals in annulus and matrix	7	Si,Al Na,Cs
1.0 SiO_2	Increased number of annular regions		
4.0 Na_2O	Matrix rutile tending to equi-axed		
	Fine dark needles and equi-axed grains		Al,Si,Na
1.0 P_2O_5	Matrix rutile chains of equi-axed grains		
	Small dark grains	8	P
2.0 Fe_2O_3	Matrix rutile fine equi-axed grains (about 1 µm across	9	
	Fine dark grains and needles		Al
	Metallics high in Fe		Fe,Mo,Ru
0.2 SiO_2	Matrix rutile equi-axed about 2 µm	10	
1.0 Na_2O	Clumps of fine dark grains		P
1.0 P_2O_5	and larger rutile crystals		
2.0 Fe_2O_3	Metallics high in Fe		Mo,Ru,Fe

TABLE 2 (continued)

Impurity (wt%)	Microconstituents	Fig. No.	Major Elements
0.02 Cl	Matrix rutile as irregular and sharp needles		
0.05 Cl	Substantial fine porosity Matrix rutile as irregular needles		
0.10 Cl	Matrix rutile as irregular needles Some fine porosity		
0.02 F	Fine dark Al-rich crystals Matrix rutile as irregular and sharp needles		Al
0.05 F	Dark crystals	11	Al
	Substantial porosity around calcine particles and titanium (oxide) relics	12	
	Matrix rutile as sharp needles Ti seems to form prismatic crystals around voids, leaving zone depleted of the acicular morphology		
0.10 F	Fine dark Al-rich crystals		
	Severe porosity around calcine particles and titanium (oxide) relics	13	
	Matrix rutile as irregular needles	14	
	Ti forms prismatic crystals around voids, leaving zone depleted of acicular morphology		
0.02 SO_4	Some fine porosity Matrix rutile as irregular crystals		
0.05 SO_4	Matrix rutile as sharp needles		
0.10 SO_4	Matrix rutile as irregular needles		

TABLE 3
SUMMARY OF MINOR MICROCONSTITUENTS

Impurity	Microconstituent	Fig. No.	Elements Present	Possible Mineral (1)
SiO_2	Small crystals	3	Si,Al	andalusite Al_2SiO_5 sillimanite Al_2SiO_5
Na_2O	Replacement of matrix rutile - small equi-axed	4	Ti	freudenbergite $Na_2Ti_6Fe_2O_9(OH)_9$
P_2O_5	Small dark crystals	8	P	monazite, rare earth phosphate
Fe_2O_3	Replacement of matrix rutile - small equi-axed crystals	9	Ti	
F	Small crystals	11	Al	
	Prismatic crystals	14	Ti,Al	
	Small acicular crystals	4	Ti,Al,Ca	hibonite (2) $Ca(Ti,Al)_{12}O_{19}$

(1) Reference - T.J. White, R. Warren and J. Warmeant, AAEC unpublished X-ray diffraction studies.
(2) P.F. Fielding and T.J. White, private communication.

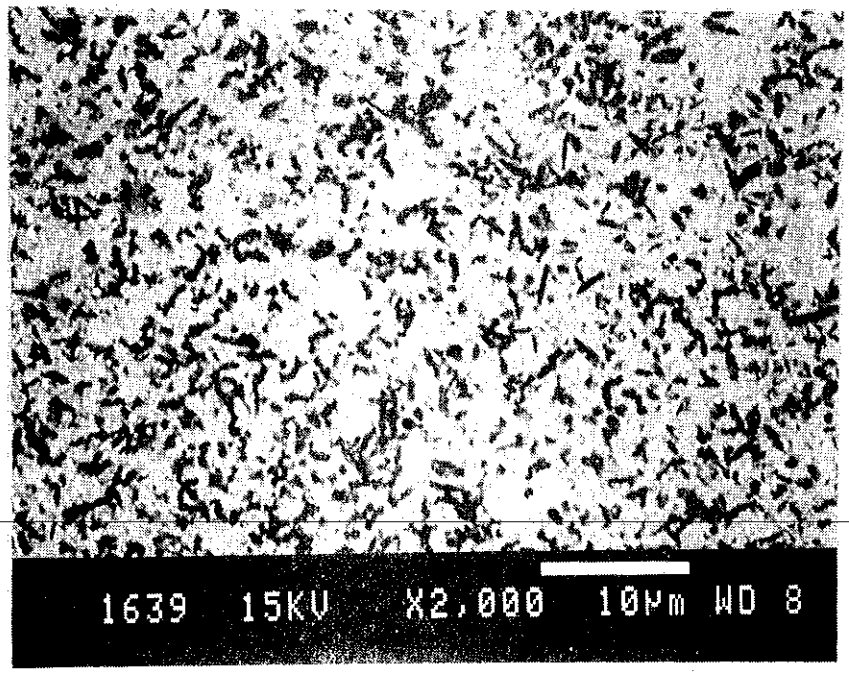

Figure 1 Typical microstructure of Synroc-C from Sandia RE 15642 precursor hot-pressed for 2 h at 1200°C. The dark acicular crystals are rutile.

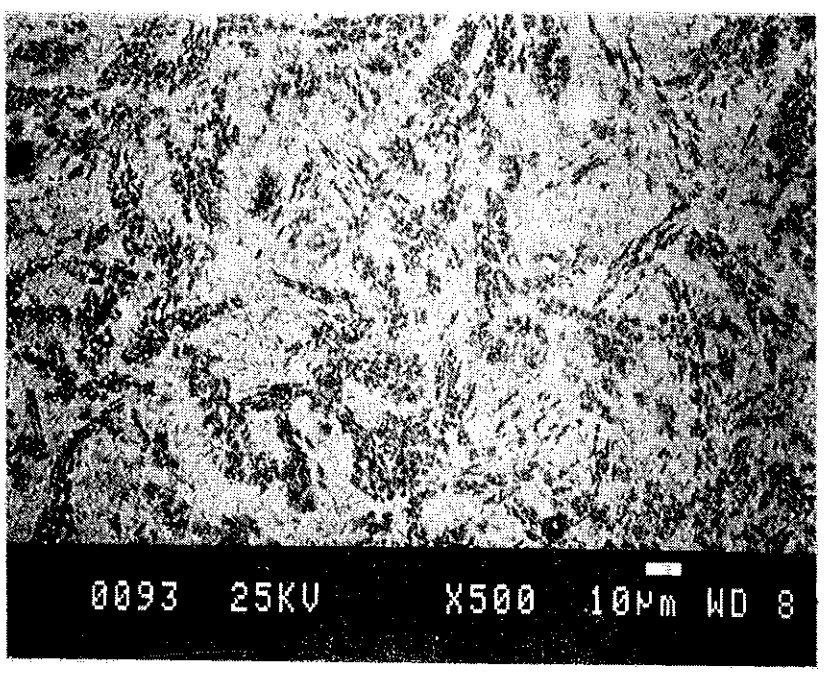

Figure 2 Microstructure of Synroc-C containing 1% SiO_2. The matrix rutile forms colonies of aligned coarse crystals typical of Synroc hot-pressed at around 1300°C.

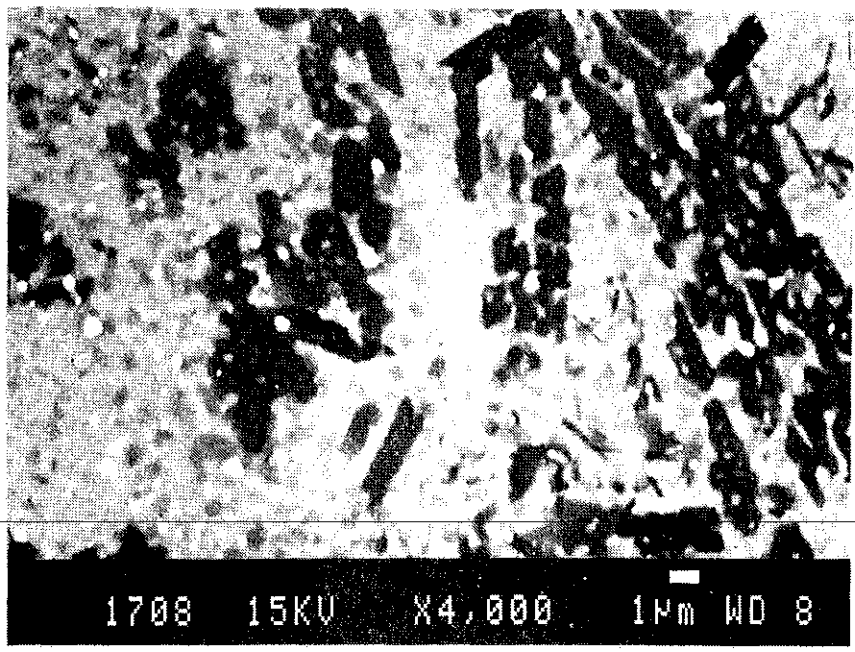

Figure 3 Dark contrast crystals of Al_2SiO_5 detected in the 1% SiO_2 specimen.

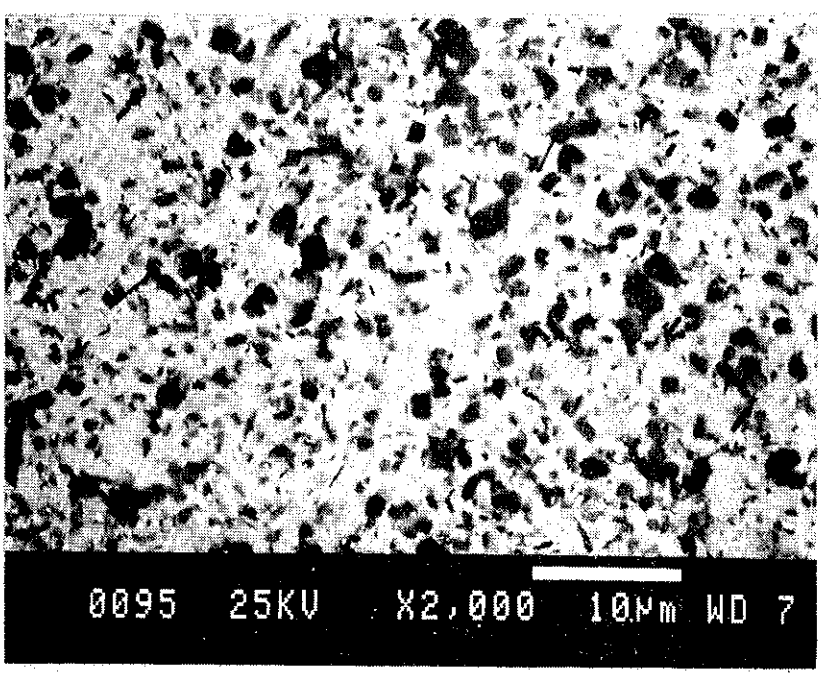

Figure 4 Microstructure of Synroc-C containing 4% Na_2O. The acicular matrix rutile has been replaced by a mixture of equi-axed Ti containing crystals and acicular calcium-aluminium titanate (hibonite).

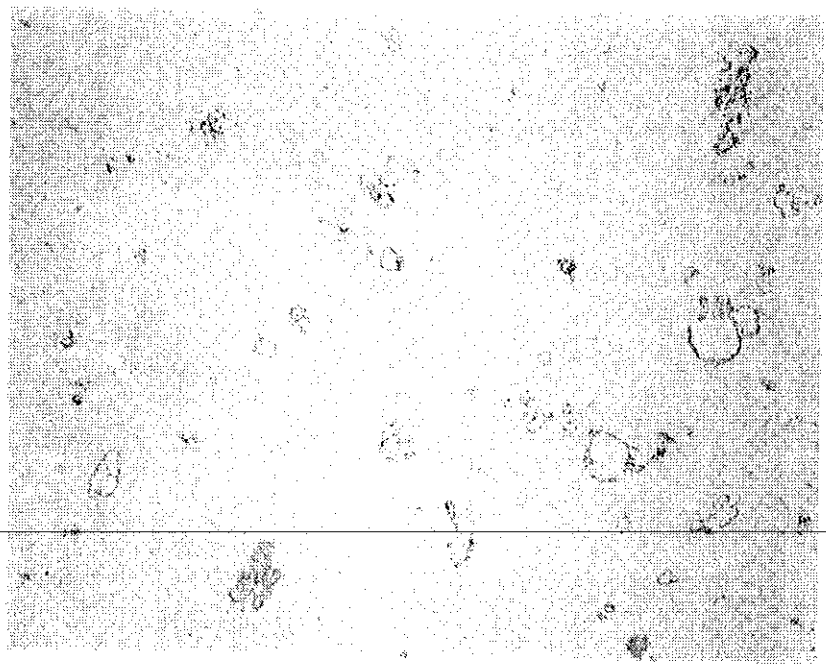

Figure 5 Optical micrograph showing Si segregations in the 0.4% SiO_2/2.5% Na_2O specimen. Magnification 100X.

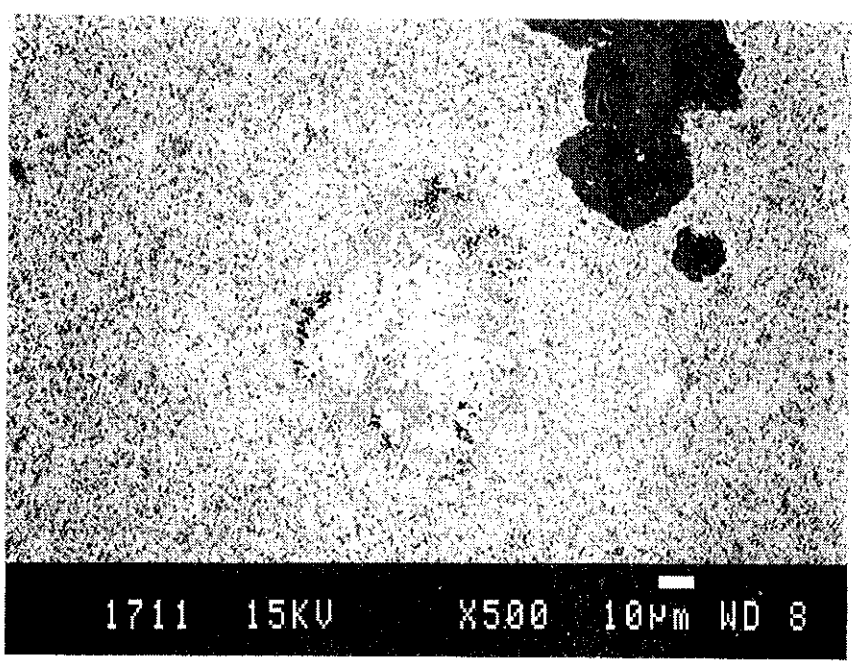

Figure 6 SEM micrograph showing Si segregation in the 0.4% SiO_2/2.5% Na_2O specimen. The high Si region is depleted of rutile but coarse rutile crystals make up the periphery. The dark globular microconstituents are oxide relics of the Ti metallic getter.

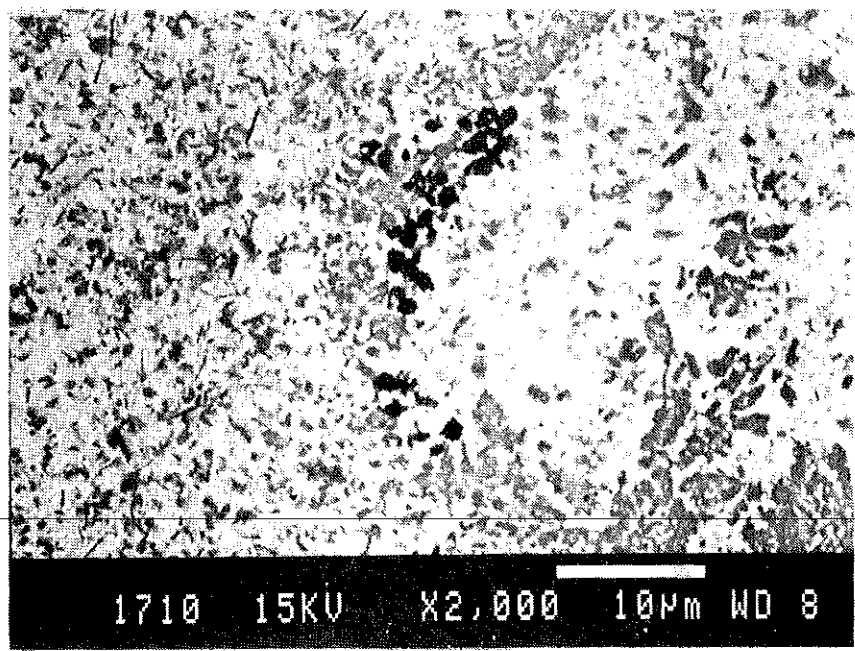

(a) 2000X

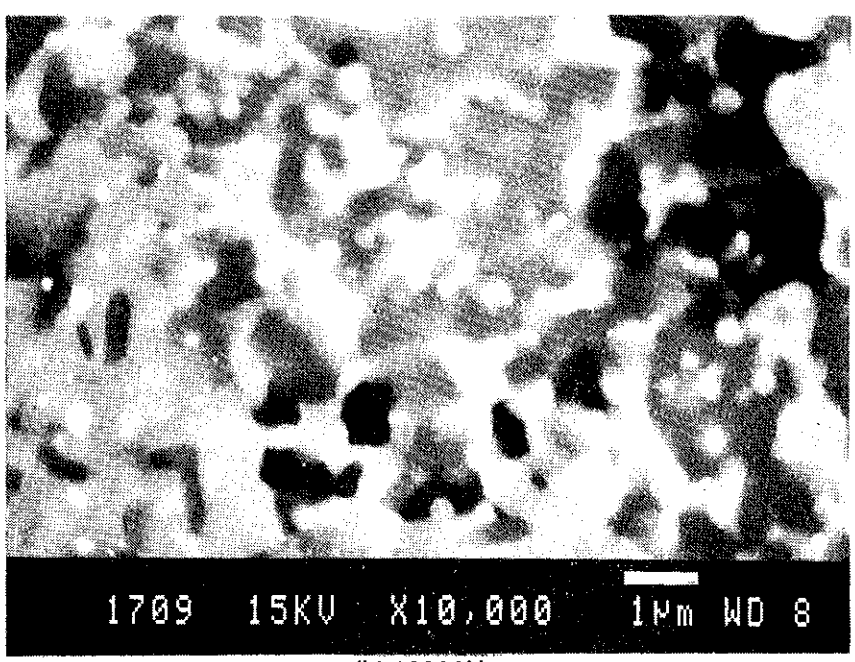

(b) 10000X

Figure 7 Detail of periphery of Si segregation showing coarse rutile crystals and fine equi-axed crystals with dark contrast.(principally Si and Al with a small amount of Na and Cs).

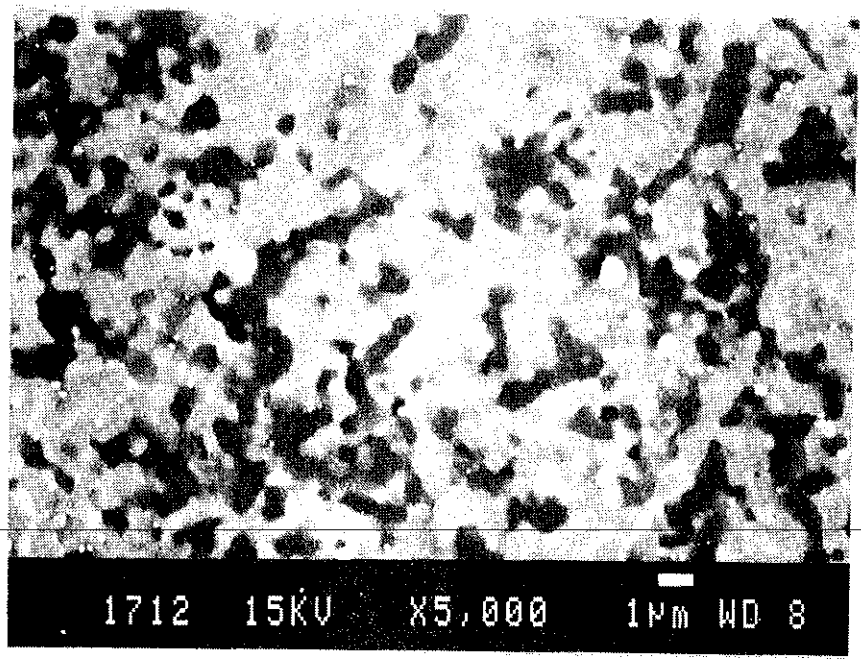

Figure 8 Small dark contrast crystals containing P detected in the specimen containing 1% P_2O_5.

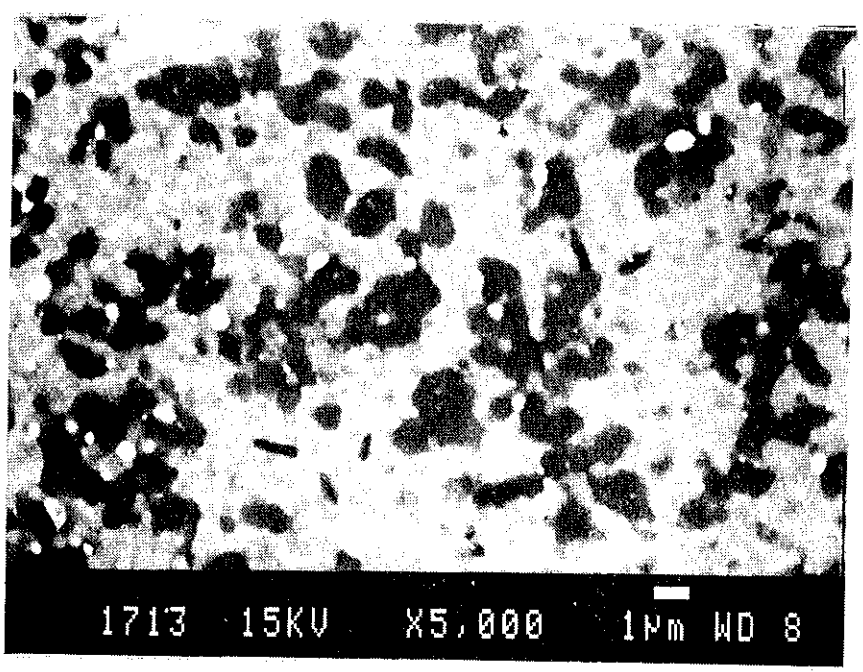

Figure 9 Equi-axed titanium(oxide) phase and trace of acicular hibonite in the specimen containing 2% Fe_2O_3.

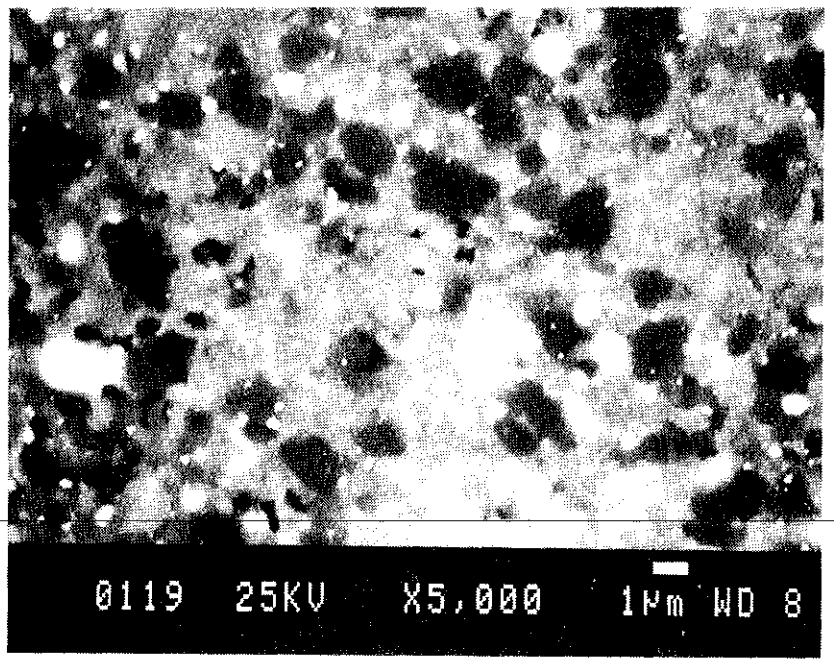

Figure 10 Microstructure of specimen containing the combination of SiO_2, Na_2O, P_2O_5 and Fe_2O_3. The fine dark crystals indicated P in the XES spectra.

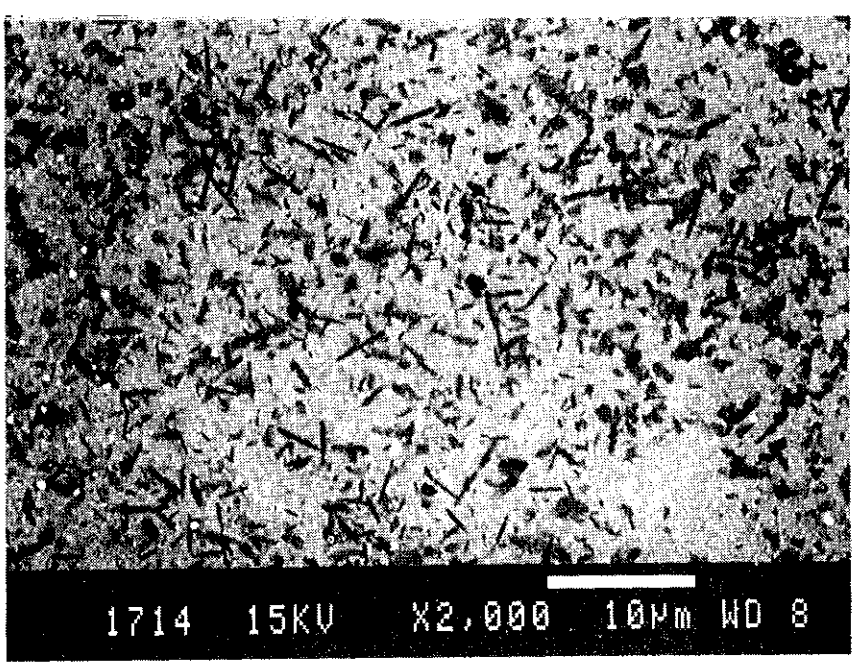

Figure 11 Dark contrast crystals high in Al, detected in specimen containing 0.05% F^-.

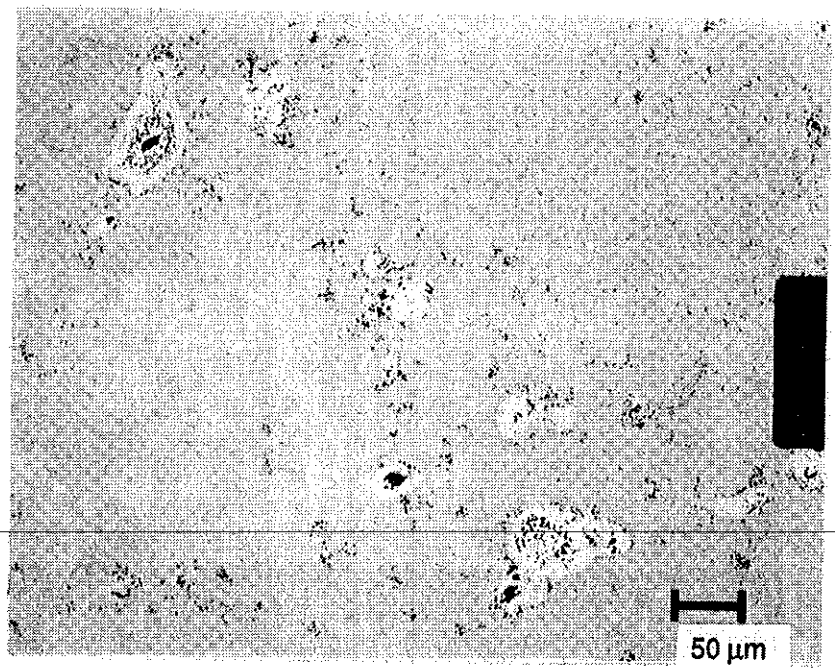

Figure 12 Optical micrograph showing substantial porosity around original calcine particles and titanium(oxide) relics in specimen containing 0.05% F^-.

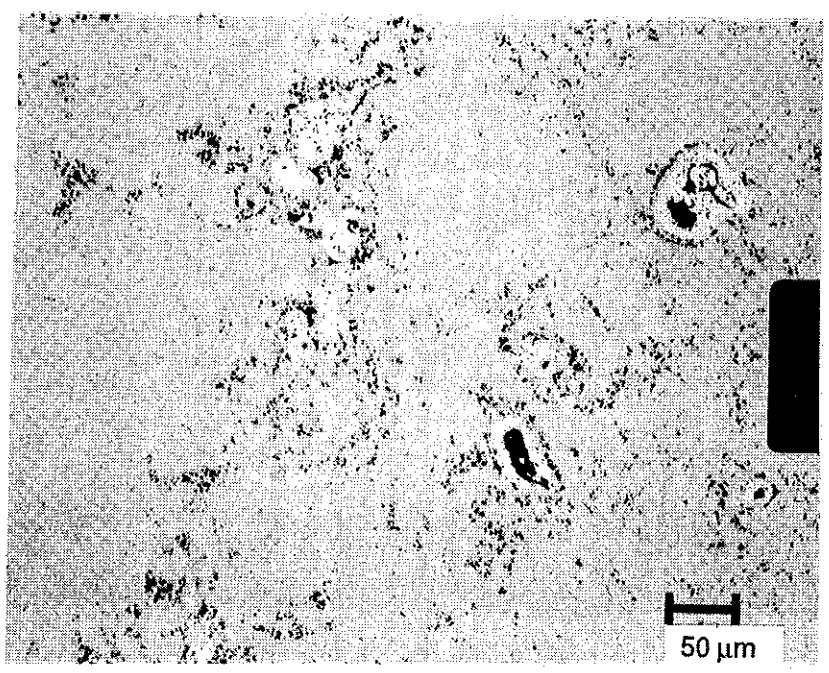

Figure 13 Optical micrograph showing severe porosity around calcine particles and titanium(oxide) relics in specimen containing 0.1% F^-.

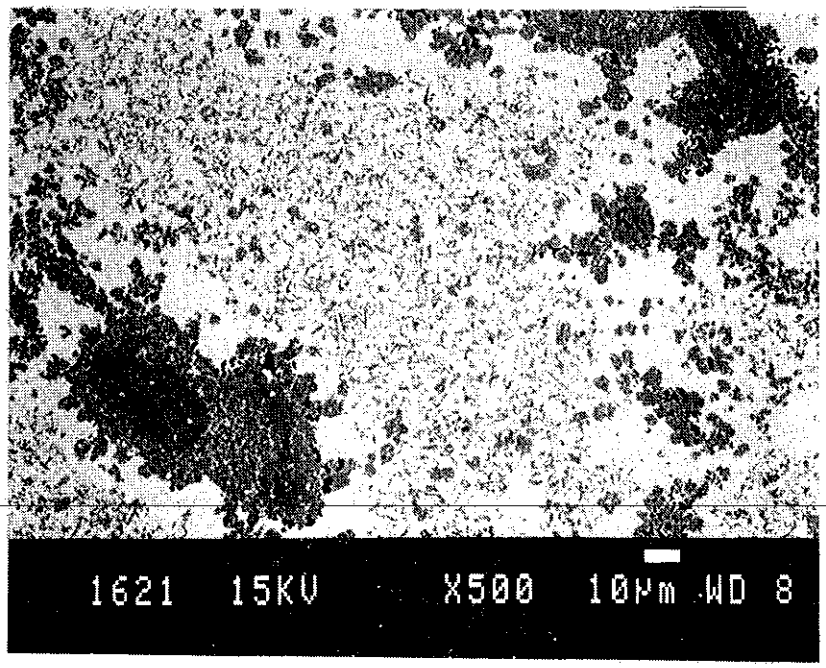

(a) Back-scattered electron image

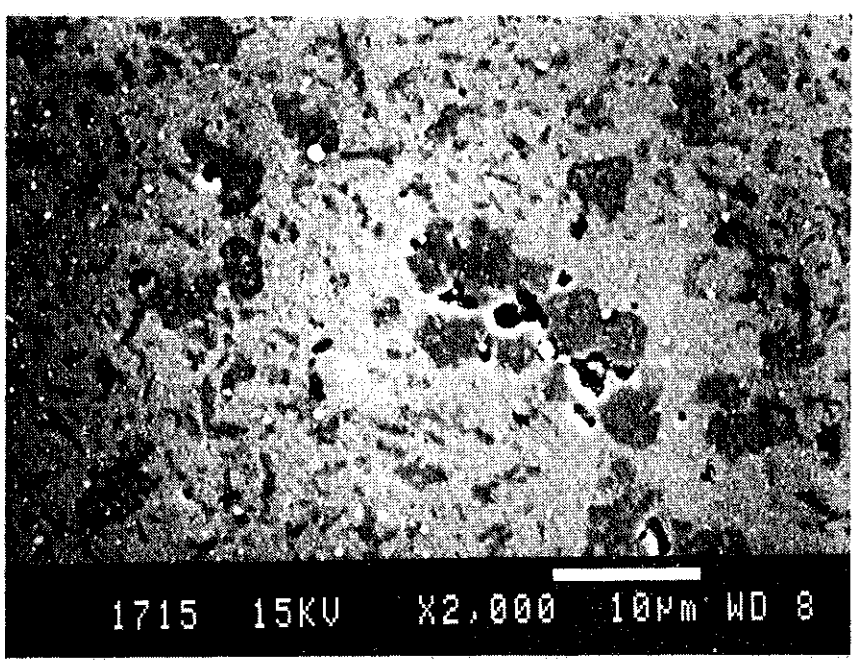

(b) Secondary electron image.

Figure 14 Micrograph from specimen containing 0.1% F showing prismatic Ti crystals associated with fine porosity.